

An experimental determination of the scale length of N₂O in the soil of a grassland

Albrecht Neftel, Andreas Blatter, and Martin Schmid

Federal Research Station of Agroecology and Agriculture, Bern, Switzerland

Bernhard Lehmann

Physics Institute, University of Bern, Bern, Switzerland

Sergei V. Tarakanov

Institute of Silicate Chemistry, St. Petersburg, Russia

Abstract. Concentration profiles of N₂O in a grassland soil and dynamic response curves to disturbance of the soil concentration (relaxation curves) were measured with a new membrane tube technique. Diffusive properties of the soil were derived from ²²²Rn measurements. The mathematical analysis of the relaxation curves yielded N₂O uptake rates U , soil diffusivities D_s , scale lengths z^* , and production rates P at different levels under the surface. The following ranges were found during 2 days of measurements: $D_s = (0.4\text{--}5) \times 10^{-7} \text{ m}^2 \text{ s}^{-1}$, $U = (1\text{--}20) \times 10^{-4} \text{ s}^{-1}$, $z^* = 0.7\text{--}2.8 \text{ cm}$, and $P = 0.02\text{--}4.4 \text{ ppt s}^{-1}$. These values were used to reproduce the measured N₂O concentration profiles with a one-dimensional diffusive transport model of N₂O in the soil air-filled pore space and to deduce flux profiles. Bidirectional fluxes occurred with small deposition fluxes up to a few ppt ms⁻¹ during intensive growing phases of the grass. Uptake rates were high enough that N₂O produced at greater depth did not reach the atmosphere.

1. Introduction

Production of N₂O in the soil occurs by nitrification and/or denitrification. Nitrification is favored under aerobic soil conditions, and N may be lost as nitric oxide (NO) as well as nitrous oxide (N₂O). A mechanism for N₂O uptake during nitrification is not known. Denitrification is favored under anaerobic conditions. With decreasing oxygen availability the production ratio $P(\text{N}_2)/P(\text{N}_2\text{O})$ increases. A net consumption of N₂O in the soil can occur in cases where the supply of oxygen to microbiologically active spots is seriously hindered or the availability of nitrate is very low [Arah and Smith, 1985; Davidson, 1991; Granli and Bøckman, 1994; Sierra et al., 1995].

In many investigations the dependence of the N₂O emissions on environmental factors and management practice has been discussed [Granli and Bøckman, 1994]. Almost all of these studies have treated soil N₂O fluxes unidirectionally; only emissions from the soil to the atmosphere have been considered, even though the distribution of the fluxes usually shows some small negative values corresponding to an uptake of N₂O. Already in 1981, Ryden [1981] published a series of N₂O exchange fluxes over a grassland that showed uptake for conditions of high soil water content and low nitrate content. The small uptake fluxes are generally not statistically significant and are therefore easily overlooked.

There is some contradiction in the literature as to the source depth of the observed N₂O emission. Many investigations dealing with agricultural soils suggest that only the first few centimeters of the soil are relevant. By far the largest part of the

emissions are observed within a few days after the application of fertilizer [Clayton et al., 1997]. Before and after this trigger event the measured fluxes are close to zero. Wienhold et al. [1995] reported N₂O fluxes between 6 and 20 ppt ms⁻¹ measured in August 1993 over a harvested wheat field in Denmark. Because of the absence of any correlation with the source area, Wienhold et al. concluded that the major contribution to the N₂O fluxes arose from soil depth below 0.9 m. The major production zone of N₂O in the deeper soil was proposed to be at the ground water level in this study. In deeper soil layers the dominant production mechanism of N₂O is likely to be denitrification, because anaerobic zones will be established in soil aggregates [Smith, 1980] and because ammonium availability and nitrification rates are low in the subsoil [Van Cleemput, 1998].

A new experimental approach was developed to find out the depth from which N₂O emitted to the atmosphere originates. Based upon a membrane tube technique this method enables the determination of the vertical N₂O profile in the soil.

2. Vertical N₂O Profiles: Scale Length

Fluxes and concentration profiles in the soil can easily be calculated for homogenous conditions, when all parameters are constant both in space and time. The vertical concentration is a solution of the diffusion equation

$$D_s \frac{d^2C}{dz^2} - UC + P = 0, \quad (1)$$

where

C N₂O concentration in the open pore space, ppt;
 z depth below the surface, m;

Copyright 2000 by the American Geophysical Union.

Paper number 2000JD900088.
 0148-0227/00/2000JD900088\$09.00

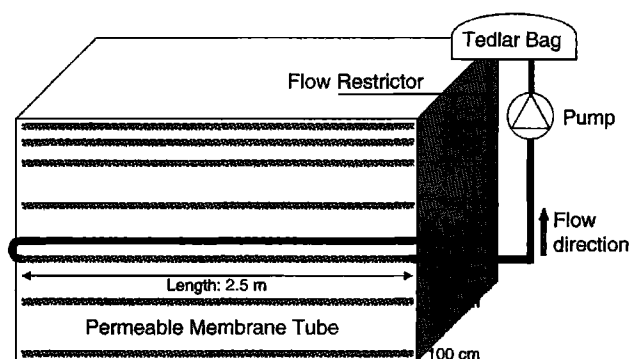


Figure 1. Setup of the installation of the permeable membrane tubes in the soil. The connection to the Tedlar bag is shown for the 50 cm depth. All tubes are sampled in parallel.

P apparent production rate of N₂O in the open pore space, ppb s⁻¹;

D_s soil diffusivity of N₂O, m² s⁻¹;

U apparent uptake rate of N₂O in the open pore space, s⁻¹.

D_s is related to the effective diffusivity D_e in the open pore space of the soil by

$$D_s \equiv \frac{\varepsilon_a D_e}{\varepsilon_a + \varepsilon_w \kappa_w + \rho K} \quad (2)$$

where

ε_a air-filled fraction of the pore space;

ε_w water-filled fraction of the pore space;

κ_w aqueous-gaseous partition coefficient of N₂O;

ρ dry bulk density of the soil;

K sorbed-gaseous partition coefficient.

Equation (1) is solved for the boundary conditions

$$C_{(z=0)} = C_0, \quad \left. \frac{dC}{dz} \right|_{z \rightarrow \infty} = 0,$$

by

$$C(z) = C_0 e^{-z/z^*} + \frac{P}{U} (1 - e^{-z/z^*}), \quad (3)$$

$$z^* = \sqrt{\frac{D_s}{U}}. \quad (4)$$

Here z^* is called the scale length and represents a natural linear scale of the adaptation of the N₂O concentration in the open pore space of the soil [Galbally and Johansson, 1989]. Below the soil-atmosphere interface the concentration is exponentially changing from the atmospheric concentration toward the equilibrium concentration C_e , the ratio of the production and the uptake rate ($C_e = P/U$). The equilibrium concentration is also known as compensation concentration [Conrad, 1994]. Here z^* is a characteristic length a N₂O molecule diffuses before it is further reduced to N₂.

In real soils neither the diffusivity, the porosity, nor the production and uptake rates are constant in space and time. As a consequence, z^* also varies with depth. When z^* substantially varies on scales of the same order as its own value, the definition of the scale length loses its meaning. N₂O fluxes are largest between layers that have differences in production and uptake rates over distances smaller than the scale length. There are two types of area where fluxes are large: in the

near-surface layer and at borders between different soil layers, e.g., at the ploughing depth. Otherwise the N₂O concentration is equal to the compensation concentration. The flux of N₂O is zero once the compensation concentration is established.

3. Experimental Setup

3.1. Membrane Tube Technique

To investigate the N₂O scale length and the soil fluxes, a new membrane tube technique [Gut et al., 1998] was implemented that allows the determination of N₂O concentrations in the open pore space of the soil. Samples for N₂O analysis were taken from 2, 5, 10, 25, 50, 70, and 100 cm depth. This technique is based on gas diffusion from the air-filled pore space in the soil into air flowing through air permeable, hydrophobic, polypropylene tubes (Accurel® PP V8/2) of 2.5 m length, horizontally installed in the soil (Figure 1). The tubes have an inner diameter of 6 mm and a mean wall thickness of 1 mm. For an air flow below 1 L min⁻¹ and a tube length of at least 1.5 m the permeation efficiency is >95%. Two different modes of sampling were used.

3.1.1. Static mode. For measuring soil profiles a closed loop through a 1 L Tedlar bag was installed. Air was pumped through the initially empty bags at a rate of 0.3 L min⁻¹ for a period of 15 min or more. A flow restrictor at the outlet of the Tedlar bag guaranteed the inflation of the bag. The N₂O concentration was measured off-line by tunable diode laser spectroscopy (Aerodyne, TDLAS 004) [Zahniser et al., 1995].

3.1.2. Dynamic mode (relaxation curves). The inlet of the membrane tube was opened at $t = 0$ to ambient air. Seven milliliter samples of air were taken at the outlet with syringes and stored in evacuated vials. The N₂O concentration was measured with a gas chromatograph (GC) (Perkin Elmer 8500 equipped with electron capture detector).

In parallel, a similar technique was used to determine effective diffusivities of soil by using ²²²Rn (B. Lehmann et al., Radon-222 monitoring of soil diffusivity, submitted to *Geophysical Research Letters*, 1999) (hereinafter referred to as Lehmann et al., submitted manuscript, 1999), a radioactive noble gas with a half-life of 3.82 days, which is produced in soils from the natural ²³⁸U decay series.

3.2. Description of the Field Site

During the vegetation period 1999, N₂O profiles in the soil of an artificial grassland with a grass-clover mixture were regularly measured to study the influence of management practice. The field is located in the Kerzersmoos 20 km northwest of Bern in the Seeland (46°59'42"N; 7°11'02"E, 436 m above sea level), a flat rural area on the Swiss plateau. The site is located in a marshland drained at the end of the 19th century. The soil is now completely mineralized with the exception of an organic layer at 60–70 cm depth. The grass was sown in autumn 1997. At the same time the membrane tubes were installed. The installation of the tubes in the soil was a major disturbance. Earlier measurements in the years 1996 and 1997 from two sets of tubes installed in the same field plot but with a time shift of six months showed that the soil under investigation needs about two months to equilibrate after the installation of the tubes. The tubes used in this study were installed in October 1997.

4. Mathematical Model for the Relaxation Curve

When the inlet of a membrane tube is opened to ambient air, the concentration at the outlet of the tube changes to a new

equilibrium value, depending on the soil diffusivity D_s , the uptake rate U , and the production rate P in the soil surrounding the membrane tube. All three parameters are assumed to stay constant during the experiment. The diffusion of N₂O molecules around the membrane tube is described by

$$\frac{\partial C_s}{\partial t} = D_s \left[\frac{1}{r} \frac{\partial}{\partial r} \left(r \frac{\partial C_s}{\partial r} \right) + \frac{\partial^2 C_s}{\partial x^2} \right] + P - UC_s, \quad (5)$$

The N₂O concentration in the membrane tube is given by

$$\frac{\partial C_t}{\partial t} + V \frac{\partial C_t}{\partial x} = -\frac{2}{R_-} F = \frac{2R_+}{R_-^2} \varepsilon_a D_e \frac{\partial C_s}{\partial r} \Big|_{r=R_-}, \quad (6)$$

where

- t time;
- r radial coordinate;
- R_- inner radius of the tube;
- R_+ outer radius of the tube;
- F flux of N₂O through the membrane wall;
- V velocity of the air flowing through the membrane tube;
- x coordinate along the tube.

The subscripts s and t denote “soil” and “tube,” respectively. Note that the diffusion term is different in (5) and (6). Equation (5) describes the diffusion in the soil that is governed by D_s , whereas (6) describes the change of the concentration in the membrane tube that is driven by the transport in the open pore space described by $(\varepsilon_a D_e)$.

The diffusive resistance of the membrane is small compared to the soil resistance and is neglected. At $t < 0$, steady state is assumed, and $C_s = P/U$. The concentration at the inlet of the tube is held constant at C_0 .

A numerical treatment of (5) and (6) allows the calculation of the outlet concentration as a function of the soil parameters (ε_a , D_e , P , and U) as well as the parameters defining the experiment (C_0 , V , and R). With a two-variable optimization routine the combination of U and $(\varepsilon_a D_e)$ that best fits the measured relaxation curve can be found. For convenience a dimensionless outlet fraction was defined as

$$\bar{C}(t) = \frac{C(t) - C_{\text{equ}}}{C_0 - C_{\text{equ}}} \quad (7)$$

where C_0 is the concentration of gas in the air inlet of the tube and C_{equ} is the new equilibrium concentration at the outlet of the tube.

The measured relaxation curve as well as the numerical simulation suggest that a new steady state is reached within a few tens of seconds. The axial diffusive flux of N₂O in the soil is small in comparison with the radial flux. Neglecting the axial flux in (5) and (6), an analytical solution for stationary conditions can be written as

$$\frac{D_s}{r} \frac{\partial}{\partial r} \left(r \frac{\partial C_s}{\partial r} \right) + P - UC_s = 0 \quad (8)$$

$$V \frac{\partial C_t}{\partial x} = -\frac{2}{R_-} F \quad 0 \leq x \leq 1 \quad (9)$$

The analytical solution for distribution of the dimensionless outlet fraction inside the tube is given by

$$\bar{C}(x) = e^{-x/X}, \quad (10)$$

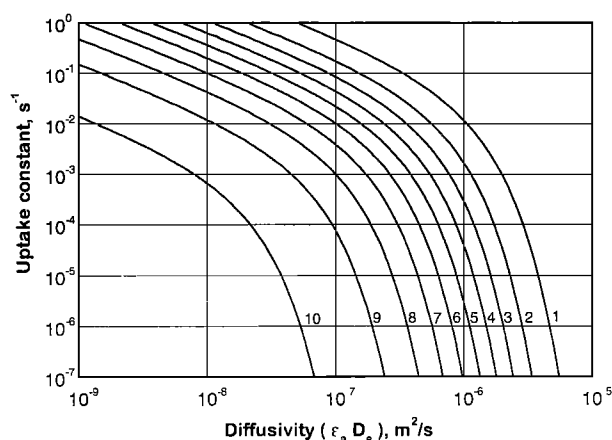


Figure 2. Calculated isopleths for the outlet fraction ranging from 0.05 to 0.95 (curves numbered 1 to 10) as function of the uptake rate and the effective diffusion coefficient, for a flow of 0.2 L min⁻¹ through a membrane tube of 2.5 m length.

$$X = \frac{VR^2 z^* K_0 \left(\frac{R_+}{z^*} \right)}{2\varepsilon_a D_e R_+ K_1 \left(\frac{R_+}{z^*} \right)}. \quad (11)$$

K_0 and K_1 are McDonald's function of zero and first order [see Janke *et al.*, 1960]. The isopleths of the outlet fraction as function of the product $(\varepsilon_a D_e)$ and the uptake rate U for the given experimental conditions (Figure 2) can be calculated from (10) and (11).

5. Results

5.1. N₂O Concentration Profiles

During the growing season of 1999 a survey of the N₂O profiles in the soil was begun. The focus was to look at effects of the cut of the grass and the application of fertilizers. Figure 3 shows five profiles taken between March 1999 and the end of May 1999, the first growing phase. The first profile taken on March 24 shows a regular increase of the concentration to the peak value of 1200 ppb at 70 cm depth, followed by a sharp decrease to values below the atmospheric concentration of 320 ppb at 100 cm depth. The concentrations measured on April 29 and March 11 are below the atmospheric concentration throughout the profiles with the lowest concentrations between 50 and 70 cm depth. The two last profiles show a strong enhancement of the N₂O concentrations in the topsoil after the cut of the grass on May 24.

5.2. N₂O Relaxation Curves

On May 27 we measured relaxation curves at 5 and 50 cm below surface. The steady state concentrations were first determined in the closed cycle mode using Tedlar bag samples. In the upper layer (5 cm) the measured N₂O equilibrium concentration was 1100 ppb (more than 3 times the atmospheric value of 320 ppb), whereas in the lower layer (50 cm) only 90 ppb was measured.

The inlet of the membrane tube was then opened to the atmosphere, and the outlet concentration was monitored by taking 7 mL samples. Figure 4 shows the relaxation curve measured in the two depths in the artificial grass field. The

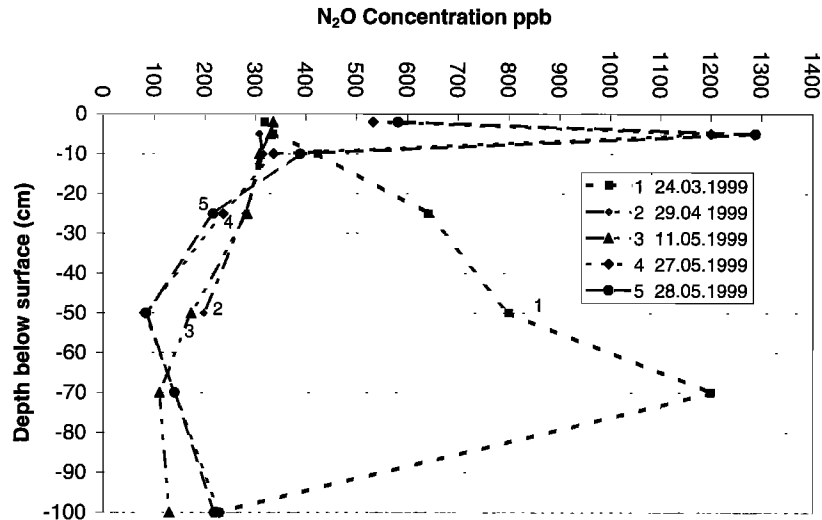


Figure 3. N₂O soil profiles from March 24, 1999, to May 28, 1999. Soil concentrations were measured at 2, 5, 10, 25, 50, 70, and 100 cm below surface with horizontally placed membrane tubes of 2.5 m length. The first cut of the grass occurred on May 24.

outlet fraction at 5 cm depth approached a value of 0.65 and at 50 cm depth approached a value of 0.85.

5.3. Determination of the Diffusivity for ²²²Rn

At 50 cm depth ($\varepsilon_a D_e$) was determined in a parallel set of tubes in the soil using the ²²²Rn method. Small amounts of atmospheric air that is essentially Rn free were injected at regular intervals into the closed loop of the Rn detector system and the membrane tube. The evaluation of the subsequent recovery of the ²²²Rn concentrations (Figure 5) allowed us to determine the diffusivity ($\varepsilon_a D_e$) in the open pore space of the soil (Lehmann et al., submitted manuscript, 1999).

D_s for ²²²Rn is connected by analogy to (2) to the relevant diffusion into the membrane tube ($\varepsilon_a D_e = \varepsilon_a D_0 \tau$).

$$D_s = \frac{\varepsilon_a D_0 \tau}{\varepsilon_a + \varepsilon_w \kappa_w + \rho K}, \quad (12)$$

where D_0 is the diffusivity in air ($1.2 \times 10^{-5} \text{ m}^2 \text{ s}^{-1}$ for Rn; $1.6 \times 10^{-5} \text{ m}^2 \text{ s}^{-1}$ for N₂O), τ is a scaling parameter reflecting the tortuous nature of the pores and the partial blocking of the pores by water (τ is the same for both gases and therefore cancels in the ratio), ε_a and ε_w are the air- and water-filled porosities, respectively, and κ_w is the aqueous-gaseous partition coefficient of the gas in water (0.29 for Rn; 0.75 for N₂O at 15°C). The factor ρK takes into account the fraction of the gas adsorbed on surfaces. For Rn a typical numerical value is 0.017 [Nazaroff, 1992], which in a first approximation, is also taken to be valid for N₂O.

The first half year of 1999 was extremely wet, and the cumulative precipitation rate in the Kerzersmoos exceeded the long-term average by 30%. The estimated water-filled porosity at 50 cm depth by the end of May was between 45 and 50%. The ratio of the diffusivity for N₂O and Rn was therefore

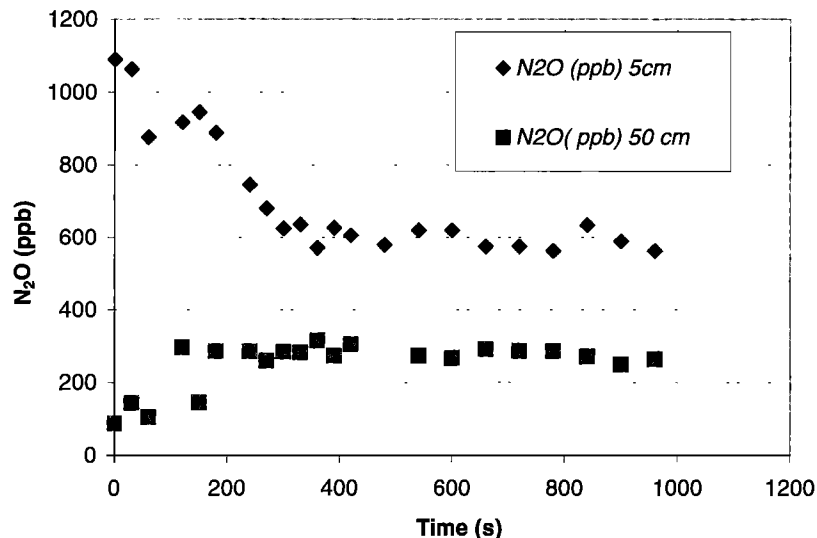


Figure 4. N₂O relaxation curves measured on May 27 at 5 cm depth and 50 cm depth.

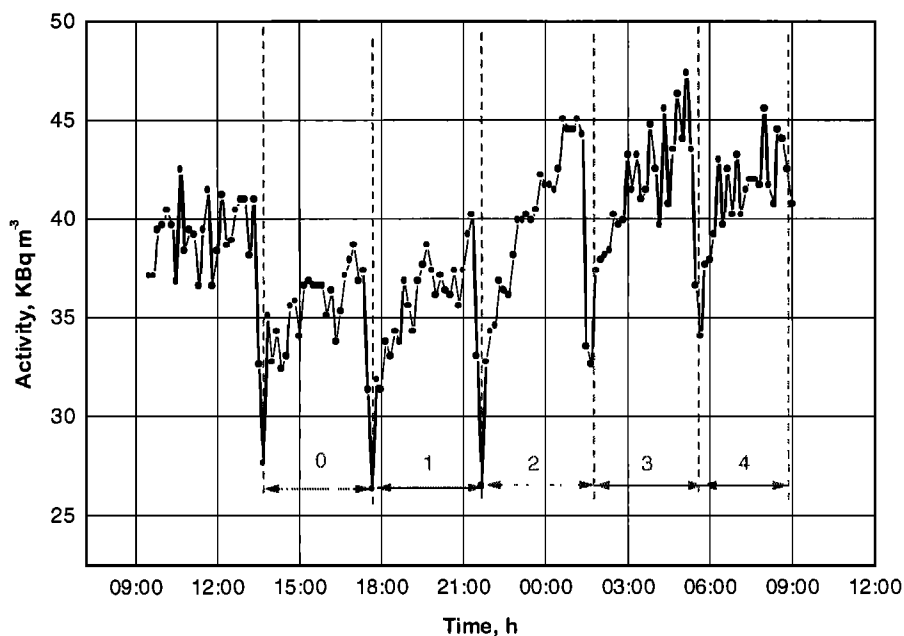


Figure 5. ²²²Rn relaxation curves from noon May 27 to noon May 28 at 50 cm depth below surface.

between 0.65 and 0.8 (Figure 6). The ratio of the effective diffusivities for Rn and N₂O only weakly depends on the factor ρK .

6. Determination of Uptake Rate U , Scale Length z^* , and Production Rate P for N₂O

Analysis of the ²²²Rn profile data for 5 cm depth yielded a range of the diffusivity $\varepsilon_a D_e$ for N₂O between $1 \times 10^{-7} \text{ m}^2 \text{ s}^{-1}$ and $2 \times 10^{-7} \text{ m}^2 \text{ s}^{-1}$. For 50 cm a range of $4 \times 10^{-8} \text{ m}^2 \text{ s}^{-1}$ to $8 \times 10^{-8} \text{ m}^2 \text{ s}^{-1}$ was derived from the ²²²Rn recovery curves (Figure 5). Knowing the diffusivities, the uptake rates U for the two depths can be determined from Figure 2 (isopleths). The relaxation curve measured at 5 cm depth has a “steady state”

outlet fraction of 0.65, and the one at 50 cm depth has a value of 0.85 (see Figure 4).

For the upper layer a value for U between $6 \times 10^{-4} \text{ s}^{-1}$ and $4 \times 10^{-3} \text{ s}^{-1}$ and for the lower layer between $2 \times 10^{-4} \text{ s}^{-1}$ and $1 \times 10^{-3} \text{ s}^{-1}$ results. This translates into a scale length z^* between 0.7 and 2.6 cm for $z = 5 \text{ cm}$ and between 0.9 and 2.8 cm for $z = 50 \text{ cm}$.

Assuming that the measured initial concentrations at the two depths represent equilibrium values, the production rate can be calculated from $P = C_e U$. For $z = 5 \text{ cm}$ the corresponding range is between 0.7 and 4.4 ppb s⁻¹, and for $z = 50 \text{ cm}$ it is between 0.018 and 0.09 ppb s⁻¹, assuming the soil properties given in Table 1.

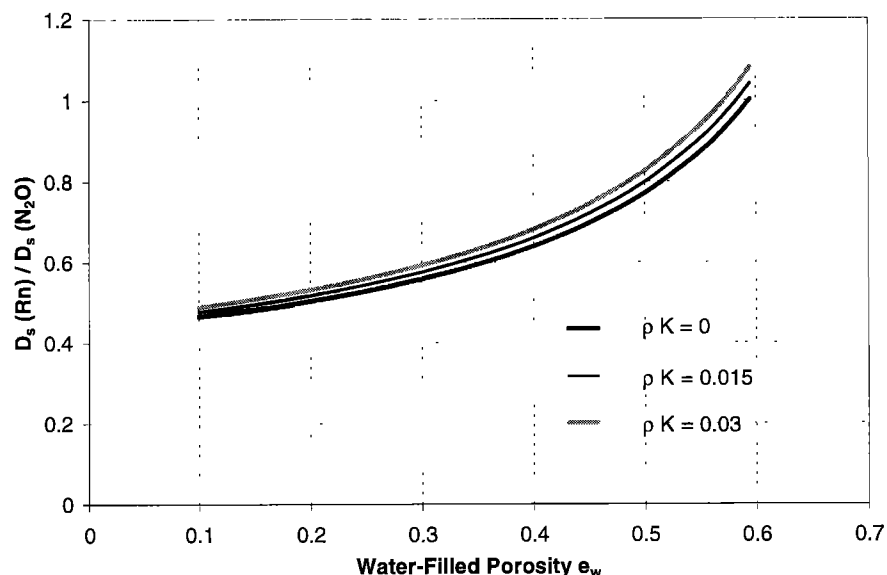


Figure 6. Ratio of the effective diffusivity of Rn and N₂O as function of the water-filled porosity with the adsorption term (ρK) varying from 0.0 to 0.034.

Table 1. Soil Properties Used for the Evaluation of ($\epsilon_a D_e$) and U From the Experimental Relaxation Curves at 5 and 50 cm Depth

	Depth	
	5 cm	50 cm
Air-filled porosity	0.17	0.17
Water-filled porosity	0.38	0.38
Aqueous-gas partition coefficient	0.75	0.75
Diffusivity in the open pore space		
$\epsilon_a D_e$, m ² s ⁻¹	1.3×10^{-7}	6.0×10^{-8}
Soil diffusivity D_s , m ² s ⁻¹	2.6×10^{-7}	1.2×10^{-7}
C_{initial} , ppbV	1100	89
$C_{\text{new steady state}}$, ppbV	600	285
Outlet fraction	0.65	0.85
Uptake rate, s ⁻¹	6×10^{-4} – 4×10^{-3}	2×10^{-4} – 1×10^{-3}
Production rate, ppb s ⁻¹	0.7–4.4	0.02–0.09
Scale length, cm	0.7–2.6	0.9–2.8

7. Discussion

7.1. N₂O Concentration Profiles

N₂O profiles (Figure 3) were measured at regular intervals during the growing season of 1999. Concentrations below the atmospheric concentration over the whole depth profile were observed in the profiles from the end of April until mid-May. The first cut of the grass occurred on May 24 and caused a mineralization pulse. The ammonium content in the first 10 cm of the soil increased from 0.35 (measured on May 17) to 2.19 ppm (measured on May 26), and the nitrate concentration increased from 1.47 to 2.11 ppm without addition of fertilizer. The soil N₂O concentration reacted immediately to the cut. In the top layer a change from a net consumption to a net pro-

duction occurred. The concentration in the layers below the ploughing depth remained below the atmospheric concentration until the end of May.

Concentrations below the atmospheric concentration signify a net consumption of N₂O in the corresponding soil layer. N₂O soil concentrations significantly below the atmospheric concentration were repeatedly seen in spring from 1997 to 1999 in the artificial grassland. Water-filled pore space varied between 50 and 90% of the total pore space. This finding contradicts the general picture that net consumption of N₂O only occurs at very high water contents [Davidson, 1991]. The rooting system and the exchange of available carbon by the grass species seem to enhance the anaerobic fraction in the pore space.

7.2. Relaxation Curves and Scale Length

The range of the evaluated scale length is between 0.7 and 3 cm. These values are taken from the isopleth curves (Figure 2), the steady state outlet fraction of the relaxation curves (Figure 4), and the effective diffusivities derived from the ²²²Rn data. U and ($\epsilon_a D_e$) can also be directly estimated from the experimentally determined relaxation curves by a two-way optimization fit as shown in Figure 7. The fits are not very good at the beginning of the curves. The experimentally determined relaxation curves increase more slowly than the calculated curves. This is mainly due to the mixing that occurs in the connections between the membrane tubes in the soil and the inlet and outlet, respectively.

The shapes of the N₂O soil concentration profiles from May 27 and 28 also support a small scale length that corresponds to the higher uptake rate. The profiles are essentially not changing from May 27 to May 28. The lower limit of the uptake rate of $6 \times 10^{-4} \text{ s}^{-1}$ corresponds to a lifetime of 33 min. In this time the mean displacement length due to diffusion is 2 cm, and the profile should be much flatter than effectively mea-

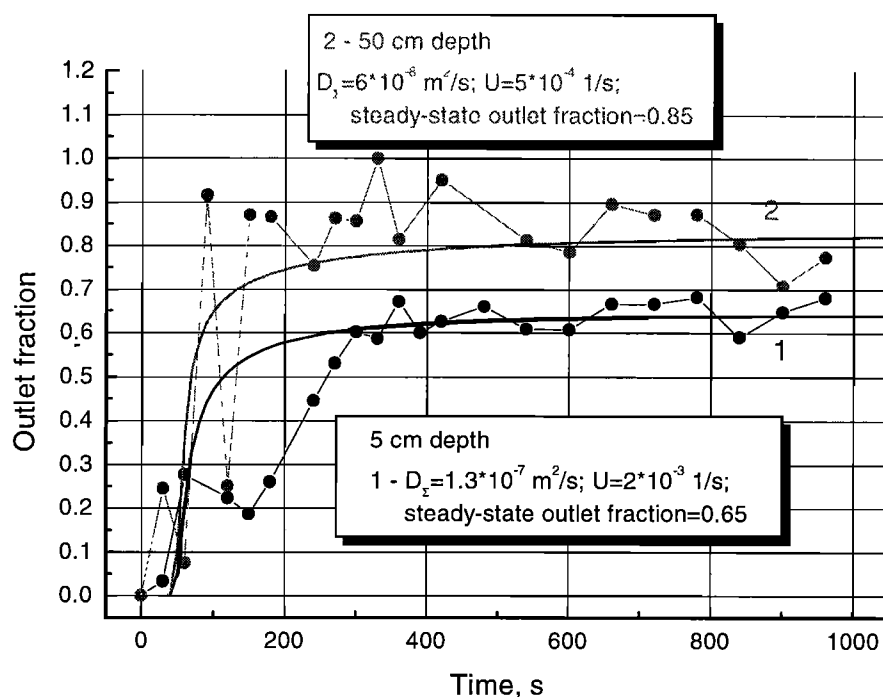


Figure 7. Measured and modeled outlet fraction of the relaxation curves from May 27 as a function of time. Curve 1: 5 cm depth; $\epsilon_a D_e = 1.3 \times 10^{-7} \text{ m}^2 \text{ s}^{-1}$; $U = 2 \times 10^{-3} \text{ s}^{-1}$; steady state outlet fraction is 0.65. Curve 2: 50 cm depth; $\epsilon_a D_e = 6 \times 10^{-8} \text{ m}^2 \text{ s}^{-1}$; $U = 5 \times 10^{-4} \text{ s}^{-1}$; steady state outlet fraction is 0.85.

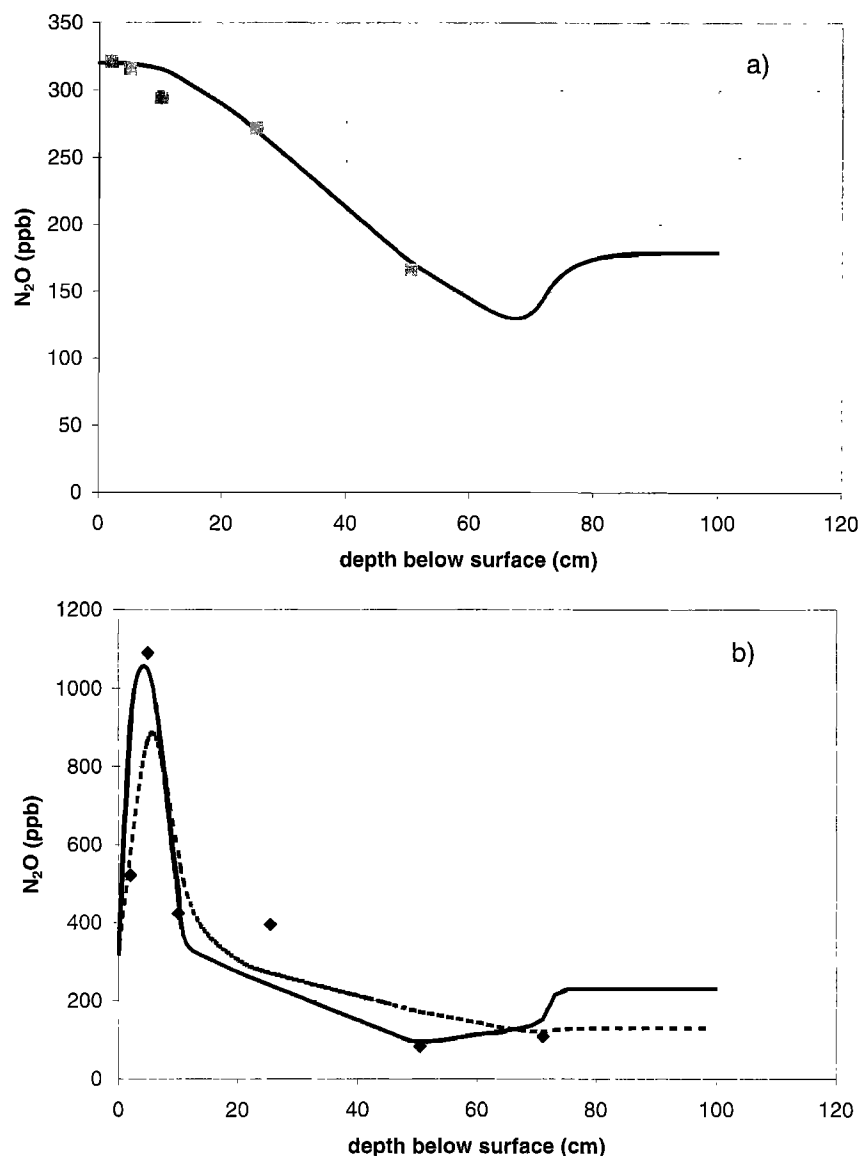


Figure 8. Calculated and measured concentration profiles for (a) May 11 and (b) May 27. The profiles from May 27 have been calculated for both the lower and the higher uptake rates as determined from the relaxation curves.

sured. Figure 8b shows the calculated profiles with an uptake rate of $6 \times 10^{-4} \text{ s}^{-1}$ (dashed curve) and $4 \times 10^{-3} \text{ s}^{-1}$ (solid curve). The curve with the lower uptake rate considerably underestimates the measured concentration at 5 cm depth below surface.

7.3. Calculated N₂O Flux Profiles in Soil

We have chosen a purely physical approach to describe the N₂O exchange in the soil and between the soil and the atmosphere. A similar approach has already been published by *Yoh*

Table 2. Values of Diffusivity and Productivity and Uptake Rates of N₂O in the Soil Used to Calculate Flux and Concentration Profiles

Layer, cm	$D_s, \text{ m}^2 \text{ s}^{-1}$		Productivity, ppb s^{-1}		Uptake, s^{-1}	
	May 11, 1999	May 27, 1999	May 11, 1999	May 27, 1999	May 11, 1999	May 27, 1999
0–4	5.0×10^{-7}	1.0×10^{-7}	1.54	2.2	4.8×10^{-3}	2.0×10^{-3}
4–7	3.0×10^{-7}	1.0×10^{-7}	1.54	2.2	4.8×10^{-3}	2.0×10^{-3}
7–15	1.5×10^{-7}	1.0×10^{-7}	1.2	3.0	3.8×10^{-3}	8.9×10^{-3}
15–40	1.0×10^{-7}	8.0×10^{-8}	0.284	0.236	1.0×10^{-3}	1.0×10^{-3}
40–60	1.0×10^{-7}	6.0×10^{-8}	0.173	0.09	1.0×10^{-3}	1.0×10^{-3}
60–85	1.0×10^{-7}	6.0×10^{-8}	0.011	0.14	1.0×10^{-4}	1.0×10^{-3}
85–100	1.0×10^{-7}	6.0×10^{-8}	0.013	0.23	1.0×10^{-4}	1.0×10^{-3}

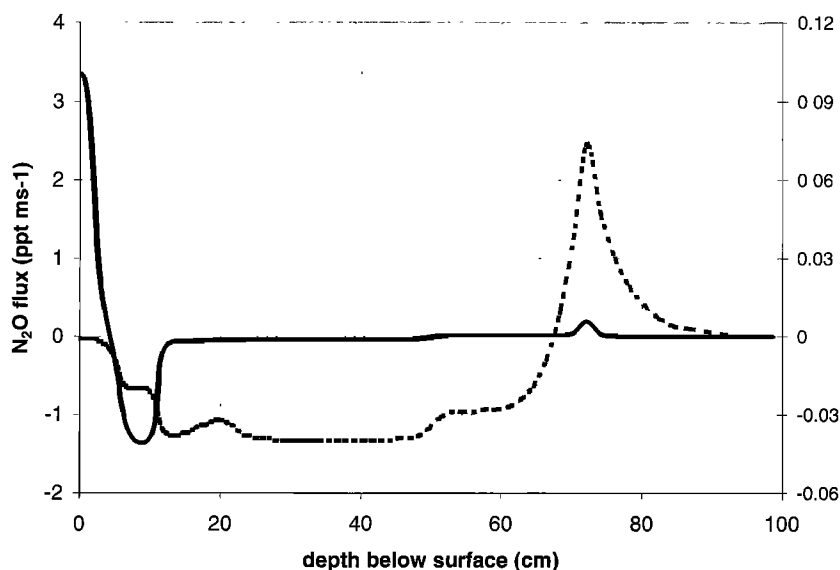


Figure 9. Calculated flux profiles. The profiles of D_{eff} and the production and uptake rates have been linearly interpolated from the values given in Table 2. The profile from May 11 is the dashed curve and corresponds to the right-hand axis; the solid curve is the profile for May 27 and corresponds to the left-hand axis. Emission fluxes are positive.

et al. [1997]. They derived the N₂O emission flux from N₂O soil profiles, water content, and soil porosity.

In this approach the N₂O depth profile is calculated as a function of production rate, uptake rate, and diffusivity. The effective diffusivity is determined by the porosity of the soil and the water-filled pore space (WFPS) and is therefore most influenced by the water exchange (rain intensity and evaporation losses) and the mechanical treatment of the soil (compaction). Production and uptake rates are determined by a cascade of interrelated processes among which the availability of substrates for nitrification (ammonium) and denitrification (nitrate) and the availability of oxygen are the most important ones [e.g., Williams *et al.*, 1992]. We selected for the analysis the profiles from May 11 and 27.

Table 2 shows the parameters selected to calculate concentration and flux profiles shown in Figures 8 and 9. On May 11, N₂O was taken up by the grassland. The flux was only on the order of 10^{-2} ppt ms⁻¹ because of the small gradient between the atmosphere and the top soil layer and the reduced transport capacity in the soil. With the first cut on May 24 the plants ceased to take up ammonium and nitrate, and an increase of the ammonium and nitrate concentrations was caused by enhanced mineralization. The increase of the substrates for nitrification and denitrification together with the reduction of the uptake by the plants is responsible for the increase of the N₂O concentration in the upper soil layers. In the zone below the plough depth the concentrations remained below the atmospheric concentration. Grass species are not rooting to these depths, and mineralization has probably not changed due to the cutting. The flux profile of May 27 shows that N₂O was emitted at a rate of the order of 1 ppt ms⁻¹ from the first few centimeters of the soil, whereas deeper down, N₂O was slowly diffusing to the layers around 50 cm.

8. Conclusions and Outlook

Sampling of soil gas with the membrane tube technique enables the determination of the parameters which describe

the N₂O flux profile in the soil. The investigated artificial grassland with a four-species grass-clover mixture shows bidirectional exchange of N₂O. Especially during the first growth period, a small but longer-lasting uptake of N₂O up to a few ppt ms⁻¹ is present. Enhanced mineralization after the first cut leads to a change from uptake to emission of N₂O from the top soil layers.

The scale length z^* is on the order of a few centimeters in the investigated soil. N₂O produced at lower depths, e.g., at the ground water level, will not reach the surface. The technique is well suited to monitor N₂O exchange fluxes in different soil systems, especially if the analytical detection system can be continuously operated on-line.

Acknowledgments. We thank two unknown reviewers for their very valuable comments. We are grateful to Deidre Belle-Oudry from the Department of Hydrology and Water Resources from the University of Arizona, Tucson, for the careful language editing. We thank Elisabeth Wälti and Elisabeth Santschi for measuring the GC samples. This work was supported by the Swiss National Science Foundation and the University of Bern. It is part of a Swiss collaboration within BIATEX-2 (Biosphere-Atmosphere-Exchange) of the European Environmental Research Programme. Financial support through KTI (project 4137.1) is greatly acknowledged.

References

- Arah, J. R. M., and K. A. Smith, Steady-state denitrification in aggregated soils: A mathematical model, *J. Soil Sci.*, **40**, 139–149, 1985.
- Clayton, H., I. P. McTaggart, J. Parker, L. Swan, and K. A. Smith, Nitrous oxide emissions from fertilised grassland: A 2-year study of the effects of N fertiliser form and environmental conditions, *Biol. Fertil. Soils*, **25**, 252–260, 1997.
- Conrad, R., Compensation concentration as critical value for regulating the flux of trace gases between soil and atmosphere, *Biogeochemistry*, **27**, 155–170, 1994.
- Davidson, E. A., Fluxes of nitrous oxide and nitric oxide from terrestrial ecosystems, in *Microbial Production and Consumption of Greenhouse Gases: Methane, Nitrogen Oxides and Halomethanes*, edited by J. E. Rogers and W. B. Whitman, pp. 219–235, Am. Soc. for Microbiol., Washington, D. C., 1991.

- Galbally, I. E., and C. Johansson, A model relating laboratory measurements of rates of nitric oxide production and field measurements of nitric oxide emissions from soils, *J. Geophys. Res.*, *94*, 6473–6480, 1989.
- Granli, T., and O. C. Bøckman, Nitrous oxide from agriculture, *Norw. J. Agric. Sci. Suppl.*, *12*, 1994.
- Gut, A., A. Blatter, M. Fahrni, B. E. Lehmann, A. Neftel, and T. Staffelbach, A new membrane tube technique (METT) for continuous gas measurements in soils, *Plant Soil*, *198*, 79–87, 1998.
- Janke, E., F. Emde, and F. Lösch, *Tafeln Hoherer Functionen*, 6th ed., B. G. Teubner Verlagsges., Stuttgart, Germany, 1960.
- Nazaroff, W. W., Radon transport from soil to air, *Rev. Geophys.*, *30*, 137–160, 1992.
- Ryden, J. C., Nitrous oxide exchange between a grassland soil and the atmosphere, *Nature*, *292*, 235–237, 1981.
- Sierra, J., P. Renault, and V. Valles, Anaerobiosis in saturated soil aggregates: Modelling and experiment, *Eur. J. Soil Sci.*, *46*, 519–531, 1995.
- Smith, K. A., A model of the extent of anaerobic zones in aggregated soils, and its potential application to estimates of denitrification, *J. Soil Sci.*, *31*, 263–277, 1980.
- Van Cleemput, O., Subsoils: Chemo- and biological denitrification, N₂O and N₂ emissions, *Nutrient Cycling Agroecosystems*, *52*, 187–194, 1998.
- Wienhold, F. G., M. Welling, and G. W. Harris, Micrometeorological measurement and source region analysis of nitrous oxide fluxes from an agricultural soil, *Atmos. Environ.*, *29*, 2219–2227, 1995.
- Williams, E. J., G. L. Hutchinson, and F. C. Fehsenfeld, NO_x and N₂O emission from soil, *Global Biogeochem. Cycles*, *6*, 351–388, 1992.
- Yoh, M., H. Toda, K. Kanda, and H. Tsuruta, Diffusion analysis of N₂O cycling in a fertilized soil, *Nutrient Cycling Agroecosystems*, *49*, 29–33, 1997.
- Zahniser, M. S., D. D. Nelson, J. B. McManus, and P. L. Keibarian, Measurement of trace gas fluxes using tunable diode laser spectroscopy, *Philos. Trans. R. Soc. London, Ser. A*, *351*, 371–382, 1995.
-
- A. Blatter, A. Neftel, and M. Schmid, Federal Research Station of Agroecology and Agriculture, Schwarzenburgstrasse 155, CH-3003 Bern, Switzerland. (albrecht.neftel@mbox.iul.admin.ch)
- B. Lehmann, Physics Institute, University of Bern, Sidlerstrasse 5, CH-3012 Bern, Switzerland. (lehmann@climate.unibe.ch)
- S. V. Tarakanov, ul. Telmana 44-93, St. Petersburg 193232, Russia. (sergei@svtar.spb.su)

(Received October 13, 1999; revised February 1, 2000; accepted February 4, 2000.)